Valence-Electron Density in Silicon and InSb under High Pressure by X-Ray Diffraction

Dale R. Yoder-Short, Roberto Colella, and Bernard A. Weinstein[a]
Department of Physics, Purdue University, West Lafayette, Indiana 47907

(Received 27 May 1982)

The effects of high pressure on the valence-electron density in silicon and indium antimonide are investigated by x-ray diffraction. It is found that near the transition to the metallic β-tin structure the scattering from the valence electrons sharply decreases, indicating either smearing of the bonding charges or increased anharmonicity in the thermal vibrations.

PACS numbers: 71.20.+c, 61.10.Fr, 62.50.+p

The scope of this work is to investigate the change of the valence-electron bonding charge in two tetrahedrally coordinated semiconductors, silicon and indium antimonide, as the interatomic distance is decreased by application of hydrostatic pressure. The range of pressures for each experiment was determined by the value at which the crystal under investigation transforms to the metallic β-tin structure: 125(± 5) kbar for silicon[1] and around 30 kbar for InSb.[2] The most direct technique for studying charge-density anisotropies in diamond structures is to measure x-ray reflections that would not exist for spherical atoms. Such reflections are those for which $h+k+l=4n+2$ and are called "forbidden reflections." The most important forbidden reflection is the (222) which has been extensively investigated.[3]

An earlier attempt to observe the effects of high pressure (up to 5.2 kbar) on the (222) of silicon failed to show any effect.[4] In our experiment, a double-crystal spectrometer was used, with a perfect crystal used as a monochromator, typically Si or InSb, cut parallel to (111), set for Bragg reflection. The high pressure was applied by using a diamond-anvil device developed by Piermarini and Block.[1] The samples were cut and etched in the shape of octagonal platelets, about 30 μm thick and 130 μm in diameter. Each sample was oriented with the (111) planes normal to the large surfaces, and was kept immersed in a 4:1 methanol-ethanol mixture, which is known to be fluid up to 104 kbar.[1] The problem of multiple Bragg scattering was carefully analyzed by rotating around the scattering vector a large crystal which was set for Bragg-reflection geometry. This test enabled us to determine the best geometrical conditions for avoiding multiple reflections at all pressure values. In InSb the (222) is not a forbidden reflection, because the cancellation effect between the In and Sb sublattices is not complete. It is, however, a weak reflection, mostly contributed by valence electrons, due to the similarity in electronic structure between indium and antimony ($Z=49$ and 51, respectively).

It turns out that (222) and $(\bar{2}\bar{2}\bar{2})$ in InSb are rigorously identical for the zinc-blende structure, even considering violation of Friedel's rule.[5] In general the (222) and $(\bar{2}\bar{2}\bar{2})$ are different, however, because the valence charge density is tetrahedrally distorted,[6] and therefore both reflections, (222) and $(\bar{2}\bar{2}\bar{2})$, have been monitored in this experiment, as a function of pressure, and have been considered independent sources of information.[7] Extinction was absent for both silicon and InSb, because of the low values of x-ray wavelength ($\lambda=0.71$ Å), structure factor, and thickness. The pressure values were measured from the Bragg angles at which the (111) and $(\bar{1}\bar{1}\bar{1})$ were found. The (111) was a strong and sharp reflection, relatively insensitive to pressure, until it suddenly disappeared during the phase transition at high pressure. The Bragg angle was related to a lattice parameter, and, through known values of elastic constants, to pressure.[8,9] This procedure was checked in one case using Si by measuring the wavelength shift of the R_1 fluorescence light emitted by a ruby fragment placed close to the crystal.[1] (A small Si crystal had to be used for this test.) The two methods agreed within experimental error up to 50 kbar, and the phase transition was found at the expected value, ± 2–3 kbar, which gives confidence to our method of measuring pressures. Table I gives the values of the lattice parameters at various pressures for Si and InSb. The width of the (111) and $(\bar{1}\bar{1}\bar{1})$ lines, about 25 arcsec, was taken as a parameter for characterizing hydrostatic condition. At very high pressures (> 104 kbar), or when the crystal was squeezed between the diamonds, a broadening of the (111) was taken as an indication of nonhydrostatic strain, and the experiment had to be repeated. Above 104 kbar it has been possible in some cases to remove nonhydrostatic strain by heating (50–100 °C) the high-

TABLE I. Lattice parameters at different pressures, calculated with use of data from Refs. 8 and 9.

Silicon		Indium antimonide	
Pressure (kbar)	Lattice parameter (Å)	Pressure (kbar)	Lattice parameters (Å)
0	5.43	0	6.48
17	5.40	6	6.45
85	5.30	16	6.40
125	5.25	30	6.36

pressure cell. In Fig. 1 we present a typical (222) profile at 150 kbar, with a Si(111) monochromator and a conventional x-ray tube (1.8 kW). The most recent data have been taken with a rotating-anode x-ray generator, with a power of 10 kW. No significant differences exist between the two sets of data, except for an obvious gain in intensity and a consequent reduction in collection times.

The data of interest are presented in Figs. 2 and 3. What is plotted in these figures are integrated intensities of the (222) reflection [and $(\bar{2}\bar{2}\bar{2})$ for InSb] as a function of pressure. All measurements are referred to the initial value measured at zero pressure. In each figure several runs are presented, corresponding to different samples, and different experimental conditions, such as choice of monochromator crystal and x-ray generator (sealed tube and rotating anode). Since the phase transition at high pressure is irreversible, a new sample was needed for each run. The first obvious feature present in all data is the poor reproducibility from run to run. At any given pressure the reproducibility was painstakingly checked by taking the high-pressure cell off the diffractometer, and putting it back. Then all the orientation procedures, including search of the umweg-free[10] region, etc., were repeated. The direct beam off the monochromator was also checked systematically. We estimate conservatively that all the points of Figs. 2 and 3 are reproducible *at the same pressure* within $\pm 2\%$, about the size of the symbols. We believe that the lack of reproducibility observable in the data is not due to accidental effects, but rather to intrinsic factors inherent in the process of changing the valence-electron density by varying the interatomic distance. For example, it has been observed that quite often the intensities could not be reproduced at a given pressure p_0 if the pressure was raised to a higher value and then decreased to the starting value p_0.

Despite poor reproducibility, some basic features clearly emerge from our data. In silicon, there is a trend in all runs for the (222) to *in-*

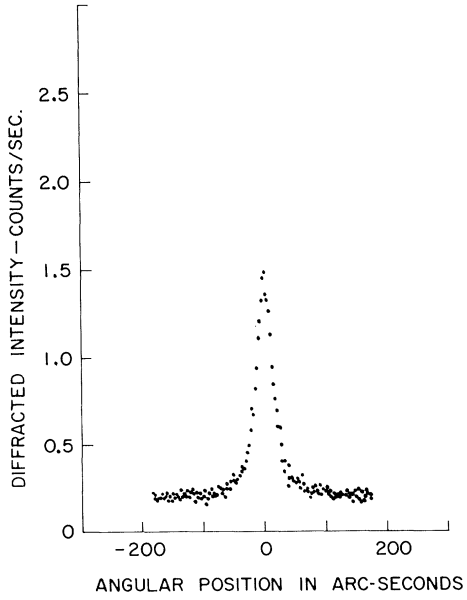

FIG. 1. Typical (222) diffraction profile from a Si crystal under high pressure (105 kbar). First crystal: (111) silicon.

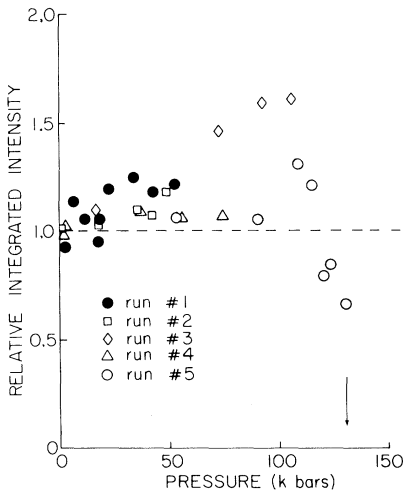

FIG. 2. Experimental plot of the relative (222) integrated intensity of Si as a function of pressure. Since run No. 5 was started at 53 kbar, the first point of the run was forced to match that of No. 4 at 53 kbar. The arrow corresponds to the disappearance of (111) at the phase transition to the metallic β-Sn structure.

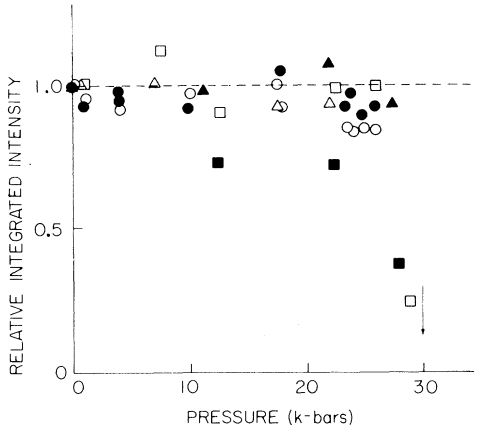

FIG. 3. Experimental plot of the relative (222) and $(\bar{2}\bar{2}\bar{2})$ integrated intensities of InSb as a function of pressure. The arrow corresponds to the phase transition. Open symbols are for (222), closed symbols are for $(\bar{2}\bar{2}\bar{2})$. Triangles, squares, and circles, refer to different independent runs.

crease before the transition. An increase in the (222) means that the covalent charge pileup between bonds is increased as the lattice parameter is decreased. In InSb the situation is less clear. If anything, there seems to be a decrease of intensity. *In both cases, in silicon and InSb, a sharp decrease is noticeable just before the structural transition.* These sharp decreases have been observed when the crystal was still entirely in the diamond structure, as evidenced by the fact that the (111) was always found sharp and equally intense right up to the transition. These results show that the time-averaged valence charge density abruptly acquires more spherical symmetry just prior to the structural change, while the crystal is still well in the tetrahedral structure. This could be due either to a smearing of the bonding charges, or to an enhancement of phonon anharmonicity which is known to cause x-ray scattering 180° out of phase with respect to that due to interatomic charge pileup.[11] The first possibility is consistent with the metallic nature of the high-pressure phase, and seems more likely at the outset. The second cannot be discounted because these solids are known to exhibit considerable anharmonicity at high pressures. We note that low-frequency zone-boundary TA modes soften under compression at a rate that has been correlated with the phase transition pressure.[12] It is suggested that recent *ab initio* pseudopotential calculations[13] could be used to resolve this issue. It is hard to say, at this stage, what are the predictions of band theory. The only band-structure calculation of F_{222} versus lattice parameter, for diamond structures, available in the literature is for carbon (diamond)[14] and shows an *increase* with pressure, in qualitative agreement with our observations. The electronic structure of Si for a pressure near the phase transition has been recently calculated using a nonspherical local pseudopotential.[15] No structure factors are calculated, but the valence pseudocharge density maps calculated near the transition pressure clearly show a decrease of valence charge at the midpoint of the bond, and a general trend to a more uniform electron density, which agrees with a *decrease* in the (222) intensity, and therefore with our results. We are not in a position, at this stage, to make any firm statement to explain the intensity drops observed in the (222) intensity near the transition pressure in silicon and indium antimonide.

This work has been supported by the National Science Foundation under Grant No. DMR-8108337 and by the National Science Foundation–Materials Research Laboratory under Grant No. DMR-8020249. This paper is based on research performed by D. R. Yoder-Short as a partial fulfillment of the requirements for the Ph.D. degree in Physics at Purdue University.

---

[a]Present address: Xerox Webster Research Center, Webster, N.Y. 14580.

[1]S. Minormura, G. A. Samara, and H. G. Drickamer, J. Appl. Phys. 33, 3196 (1962); G. J. Piermarini and S. Block, Rev. Sci. Instrum. 46, 973 (1975).

[2]B. Okai and J. Yoshimoto, J. Phys. Soc. Jpn. 45, 1880 (1978).

[3]See the review article by R. Colella, Phys. Scr. 15, 143 (1977), and references therein.

[4]I. Fujimoto, Phys. Rev. B 9, 591 (1974).

[5]R. Colella, Phys. Rev. B 3, 4308 (1971).

[6]D. H. Bilderback and R. Colella, Phys. Rev. B 13, 2479 (1976).

[7]The (222) and $(\bar{2}\bar{2}\bar{2})$ reflections were labeled and identified according to the criteria given in Ref. 6.

[8]F. D. Murnaghan, Proc. Nat. Acad. Sci. U.S. 30, 244 (1944).

[9]For Si: *Mechanical and Thermal Properties of Ceramics*, edited by J. B. Wachtman, Jr., National Bureau of Standards Special-Publication No. 303 (U.S. GPO, Washington, D.C., 1969), p. 139. For InSb: I. O. Bashkin and G. I. Peresada, Fiz. Tverd. Tela 16, 3166 (1974) [Sov. Phys. Solid State 16, 2058 (1975)].

[10]Umweg, English abbreviation of *Umweganregung* (detour radiation). It has to do with simultaneous Bragg reflections.

[11]D. Keating, A. Nunes, B. W. Batterman, and J. Hast-

ings, Phys. Rev. B 4, 2472 (1971).
[12]B. A. Weinstein, Solid State Commun. 24, 595 (1977).
[13]M. T. Yin and M. L. Cohen, J. Phys. Soc. Jpn., Suppl. A 49, 13 (1980).
[14]A. Zunger and A. J. Freeman, Phys. Rev. B 15, 5049 (1977).
[15]V. K. Bashenov and Y. K. Markolenko, Phys. Status Solidi (b) 97, K145 (1980); V. K. Bashenov, Y. K. Markolenko, and V. V. Timofeenko, Fiz. Tverd. Tela 22, 934 (1980) [Sov. Phys. Solid State 22, 549 (1980)].

Fractal (Scaling) Clusters in Thin Gold Films near the Percolation Threshold

R. F. Voss, R. B. Laibowitz, and E. I. Allessandrini
IBM Thomas J. Watson Research Center, Yorktown Heights, New York 10598
(Received 30 June 1982)

Transmission electron micrographs of thin evaporated gold films were analyzed by computer. For length scales above 10 nm, the irregular connected clusters show a perimeter linearly proportional to area. Near the percolation threshold the large-scale power-law correlations and area distributions are consistent with the scaling theory of second-order phase transitions. Geometrically, the boundary of all clusters is a fractal of dimension $D = 2$ while individual boundaries are of fractal dimension $D_C \approx 1.9$.

PACS numbers: 71.30.+h, 05.40.+j, 61.16.Di

A random mixture of conducting (fraction p) and insulating (fraction $1-p$) material abruptly exhibits long-range conduction at a critical concentration $p = p_c$. This simple percolation problem[1] is ideally suited to computer modeling,[1-5] and mathematically equivalent to a second-order phase transition.[6] The rich variety of universal "scaling" behavior near p_c is reflected in the irregular shapes of the connected clusters. Until recently[7] statistical studies of cluster geometry were limited to computer simulations. Conversely, experimental studies of actual materials[8] have been based on conductivity measurements (in spite of the availability of micrographs). In this Letter we present detailed experimental results on the cluster geometry of thin gold films near p_c taken from digitized micrographs. Although local Au-Au and Au-substrate correlations during deposition alter p_c, we find the large-scale properties to be consistent with both scaling theory and computer simulation. Thus, the metal-insulator transition in actual films can belong to the same universality class as the idealized percolation problem.

A mature, analytic scaling theory[1] exists for the percolation transition. Power-law relationships extend over length scales that vary from the model lattice spacing to the correlation length ξ. Near p_c, ξ diverges as $|p-p_c|^{-\nu}$. The characteristic exponents, however, fail to provide an intuitively satisfying description of the intricate, seemingly biological, cluster shapes. Mandelbrot's fractal geometry,[9] on the other hand, offers a natural description in terms of the fractal dimension D of the collected cluster boundaries and the dimension D_C of an individual cluster boundary. Fractals provide an intuitive geometric basis for the scaling behavior, as well as specific geometric models[2,10] for analytic calculations. We shall, therefore, discuss our measurements in terms of both scaling theory and fractals.

The thin Au films were made at room temperature by electron-beam evaporation onto 30-nm-thick amorphous Si_3N_4 windows grown on a Si wafer frame. The deposition rate was 0.5 nm/sec at a base pressure of 2×10^{-7} Torr. Sample thickness was systematically varied with a moving shutter to produce simultaneously a range of samples from 6 to 10 nm thick that varied from electrically insulating to conducting. Transmission electron micrographs were digitized with a scanning microdensitometer (typically on a 512 $\times$ 512 grid). Figure 1(a) shows a halftone representation of one of the digitized images. The structure within each cluster is due to the Au grains. With use of threshold detection and an optimal connectivity-checking algorithm the individual Au clusters were isolated for statistical analysis. In Fig. 1(b) the three largest clusters from Fig. 1(a) are darkest while the remaining clusters are a uniform light gray. At a fractional Au coverage $p = 0.64$, Fig. 1(b) is below p_c and the extent of the largest clusters is less than the

